ORGANIC LETTERS

2013
Vol. 15, No. 1
80–83

Sequential Electrophilic and Photochemical Cyclizations from Bis(bithienyl)acetylene to a Tetrathienonaphthalene Core

Chuandong Dou, Shohei Saito, Libin Gao, Naoki Matsumoto, Takashi Karasawa, Hongyu Zhang, Aiko Fukazawa, and Shigehiro Yamaguchi*

Department of Chemistry, Graduate School of Science, Nagoya University, and CREST, Japan Science and Technology Agency, Furo, Chikusa, Nagoya 464-8602, Japan

yamaguchi@chem.nagoya-u.ac.jp

Received November 12, 2012

ABSTRACT

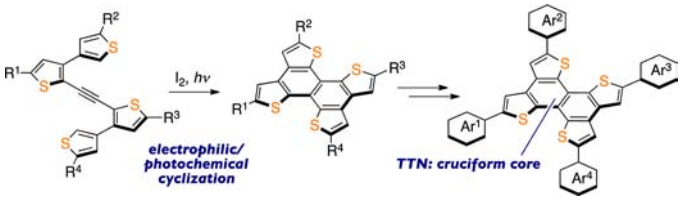

Photoirradiation of bis(bithienyl)acetylenes in the presence of iodine undergoes sequential electrophilic and photochemical cyclizations to produce tetrathienonaphthalenes (TTN) in one pot. The TTN framework is readily transformed into cruciform π-extended derivatives, which form ordered nano/microstructures.

Flat and rigid π-conjugated organic molecules have been extensively studied as promising materials for various applications including organic light-emitting diodes, organic field-effect transistors, and organic photovoltaics.[1] With the increasing demands for the two-dimensionally (2-D) extended scaffolds with intriguing electronic structures as well as favorable aggregation properties, a number of synthetic methodologies have been developed for the preparation of novel polycyclic π frameworks. The representative methods are oxidative coupling between adjacent aromatic rings such as the Scholl reaction,[2] transition-metal-catalyzed intramolecular C−H arylations,[3] and Mallory photochemical cyclization.[4] An alternative approach is the cyclization of arylacetylenes triggered by oxidants, acids, or electrophilic reagents including metal complexes.[5] In particular, bis(biaryl)acetylenes are useful precursors for the direct construction of polycyclic scaffolds (Figure 1). For example, Swager and Yamaguchi reported the oxidative cyclization of bis(biphenyl)acetylenes using $SbCl_5$ as an oxidant, which doubly undergoes an electrophilic

(1) For recent reviews of flat and rigid π-conjugated systems, see: (a) Grimsdale, A. C.; Müllen, K. *Macromol. Rapid Commun.* **2007**, *28*, 1676. (b) Zang, L.; Che, Y.; Moore, J. S. *Acc. Chem. Res.* **2008**, *41*, 1596. (c) Fukazawa, A.; Yamaguchi, S. *Chem. Asian J.* **2009**, *4*, 1386. (d) Skabara, P. J. In *Handbook of Thiophene-Based Materials*; Perepichka, I. F., Perepichka, D. F., Eds.; Wiley-VCH: Weinheim, 2009; Vol. 1, 219. (e) Takimiya, K.; Shinamura, S.; Osaka, I.; Miyazaki, E. *Adv. Mater.* **2011**, *23*, 4347. (f) Chen, L.; Hernandez, Y.; Feng, X.; Müllen, K. *Angew. Chem., Int. Ed.* **2012**, *51*, 7640.

(2) (a) Scholl, R.; Seer, C. *Justus Liebigs Ann. Chem.* **1912**, *394*, 111. (b) Wu, J.; Pisula, W.; Müllen, K. *Chem. Rev.* **2007**, *107*, 718. (c) King, B. T.; Kroulík, J.; Robertson, C. R.; Rempala, P.; Hilton, C. L.; Korinek, J. D.; Gortari, L. M. *J. Org. Chem.* **2007**, *72*, 2279.

(3) (a) Shen, H.-C.; Tang, J.-M.; Chang, H.-K.; Yang, C.-W.; Liu, R.-S. *J. Org. Chem.* **2005**, *70*, 10113. (b) Alberico, D.; Scott, M. E.; Lautens, M. *Chem. Rev.* **2007**, *107*, 174. (c) Pascual, S.; Mendoza, P.; Echavarren, A. M. *Org. Biomol. Chem.* **2007**, *5*, 2727. (d) Yamaguchi, J.; Yamaguchi, A. D.; Itami, K. *Angew. Chem., Int. Ed.* **2012**, *51*, 8960.

(4) (a) Mallory, F. B.; Mallory, C. W. *Organic Reactions*; Wiley & Sons: New York, 1984; Vol. 30, p 1. (b) Liu, L.; Yang, B.; Katz, T. J.; Poindexter, M. K. *J. Org. Chem.* **1991**, *56*, 3769.

(5) (a) Larock, R. C.; Harrison, L. W. *J. Am. Chem. Soc.* **1984**, *106*, 4218. (b) Goldfinger, M. B.; Crawford, K. B.; Swager, T. M. *J. Am. Chem. Soc.* **1997**, *119*, 4578. (c) Alonso, F.; Beletskaya, I. P.; Yus, M. *Chem. Rev.* **2004**, *104*, 3079. (d) Yue, D.; Yao, T.; Larock, R. C. *J. Org. Chem.* **2005**, *70*, 10292. (e) Soriano, E.; Marco-Contelles, J. *Organometallics* **2006**, *25*, 4542. (f) Kashiki, T.; Shinamura, S.; Kohara, M.; Miyazaki, E.; Takimiya, K.; Ikeda, M.; Kuwabara, H. *Org. Lett.* **2009**, *11*, 2473. (g) Mehta, S.; Larock, R. C. *J. Org. Chem.* **2010**, *75*, 1652. (h) Godoi, B.; Schumacher, R. F.; Zeni, G. *Chem. Rev.* **2011**, *111*, 2937. (i) Hayashi, M.; Toshimitsu, F.; Sakamoto, R.; Nishihara, H. *J. Am. Chem. Soc.* **2011**, *133*, 14518. (j) VanVeller, B.; Robinson, D.; Swager, T. M. *Angew. Chem., Int. Ed.* **2012**, *51*, 1182.

10.1021/ol303107y
Published on Web 12/12/2012

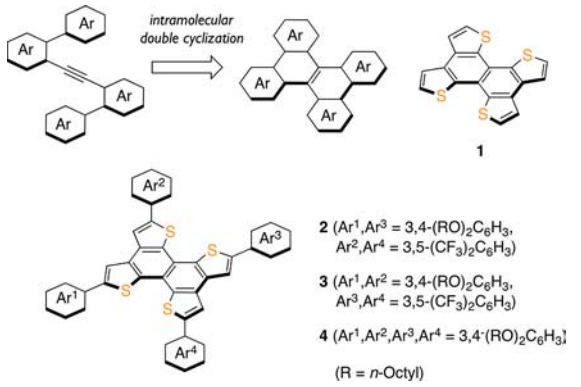

Figure 1. Direct construction of polycyclic π-scaffolds from bis(biaryl)acetylenes and a series of TTN derivatives.

cyclization in a 6-*endo* mode to produce a dibenzo[*g*,*p*]chrysene skeleton.[6] Liu and co-workers also reported sequential reactions from bis(biaryl)acetylenes combining the ICl-induced cyclization and the Pd-catalyzed coupling reaction to synthesize various polycyclic aromatic hydrocarbons, in which the first monocyclized intermediates need to be isolated.[7]

During the course of our acetylene cyclization chemistry for polycyclic π-electron materials,[8] we have now found that the photoirradiation of bis(bithienyl)acetylenes cleanly produces a tetrathienonaphthalene (TTN) skeleton **1**. The high yields and facile one-pot protocol are the advantages of this method over the conventional synthesis of the TTN skeleton.[9] The regiocontrolled functionalization can be also conducted for synthesizing more π-extended derivatives on demand. It has turned out that the TTN core is a useful 2-D scaffold as an intersection to extend π-conjugation in a cruciform fashion. With a series of tetraaryl-substituted derivatives **2**–**4** in hand (Figure 1), we have also investigated the electronic impacts of their π-extension modes as well as their aggregation properties.

A THF solution of bis(silyl)-substituted bis(3,3′-bithiophen-2-yl)acetylene **5a** with an excess amount (10 equiv) of I_2 was irradiated by a high-pressure mercury lamp at room temperature under an argon atmosphere (Scheme 1). The mixture smoothly turned into a deep brown solution. After irradiation for 50 h, the reaction mixture was quenched

Scheme 1. Double Cyclization of Bis(biphenyl)acetylene

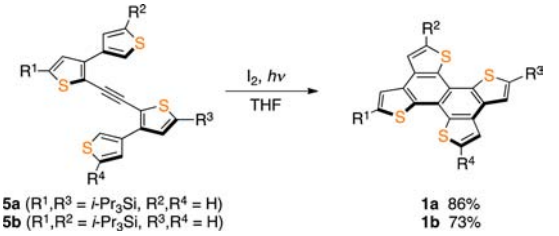

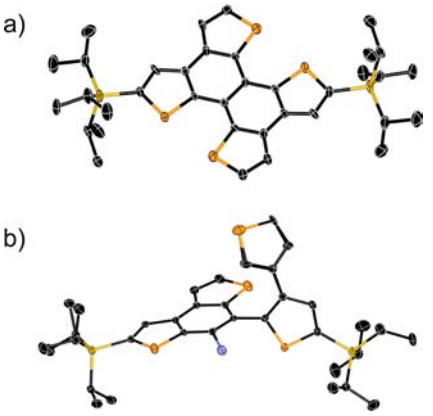

Figure 2. Crystal structures of a) **1a** and b) **6a** (50% probability for thermal ellipsoids). Hydrogen atoms are omitted for clarity.

with a saturated Na_2SO_3 aqueous solution. Recrystallization from CH_2Cl_2/hexane gave the TTN product **1a** in 86% yield. Using **5b** as a precursor, the corresponding regioisomer **1b** was also successfully synthesized in 73% yield.

The structures of **1a** and **1b** were verified by NMR spectroscopy and mass spectrometry and finally by an X-ray diffraction analysis. The crystal structures showed a completely planar geometry of the TTN skeleton (Figure 2a). While the bulky triisopropylsilyl (TIPS) groups in **1a** prevented intermolecular π-stacking, **1b** formed a π-stacked dimer with the TIPS groups oriented outside. The interfacial distance between the mean planes of the TTN cores is 3.41 Å (see the Supporting Information). These different packing structures suggest that the self-assembling mode of the TTN skeleton is controllable by incorporating substituents at the appropriate positions.

To gain insight into the mechanism of the double cyclization, the reaction of **5a** was monitored by ^{1}H NMR spectroscopy (Figure 3). After UV light irradiation for 11 h, the signals of **5a** completely disappeared and a set of new signals for an intermediate appeared together with the small signals of the double-cyclized product **1a**. When a THF solution of **5a** was stirred with I_2 even in the dark at room temperature, **5a** was gradually consumed to eventually yield the intermediate without the formation of the

(6) Yamaguchi, S.; Swager, T. M. *J. Am. Chem. Soc.* **2001**, *123*, 12087.

(7) (a) Li, C.-W.; Wang, C.-I.; Liao, H.-Y.; Chaudhuri, R.; Liu, R.-S. *J. Org. Chem.* **2007**, *72*, 9203. (b) Chaudhuri, R.; Hsu, M.-Y.; Li, C.-W.; Wang, C.-I; Chen, C.-J.; Lai, C. K.; Chen, L.-Y.; Liu, S.-H.; Wu, C.-C.; Liu, R.-S. *Org. Lett.* **2008**, *10*, 3053. (c) Mukherjee, A.; Pati, K.; Liu, R.-S. *J. Org. Chem.* **2009**, *74*, 6311. (d) Chen, T.-A.; Liu, R.-S. *Org. Lett.* **2011**, *13*, 4644.

(8) (a) Xu, C. H.; Wakamiya, A.; Yamaguchi, S. *J. Am. Chem. Soc.* **2005**, *127*, 1638. (b) Okamoto, T.; Kudoh, K.; Wakamiya, A.; Yamaguchi, S. *Chem.—Eur. J.* **2007**, *13*, 548. (c) Zhang, H.; Wakamiya, A.; Yamaguchi, S. *Org. Lett.* **2008**, *10*, 3591. (d) Fukazawa, A.; Yamada, H.; Yamaguchi, S. *Angew. Chem., Int. Ed.* **2008**, *47*, 5582.

(9) (a) Fischer, E.; Larsen, J.; Christensen, J. B.; Fourmigué, M.; Madsen, H. G.; Harrit, N. *J. Org. Chem.* **1996**, *61*, 6997. (b) Wang, Z.; Shi, J.; Wang, J.; Li, C.; Tian, X.; Cheng, Y.; Wang, H. *Org. Lett.* **2010**, *12*, 456.

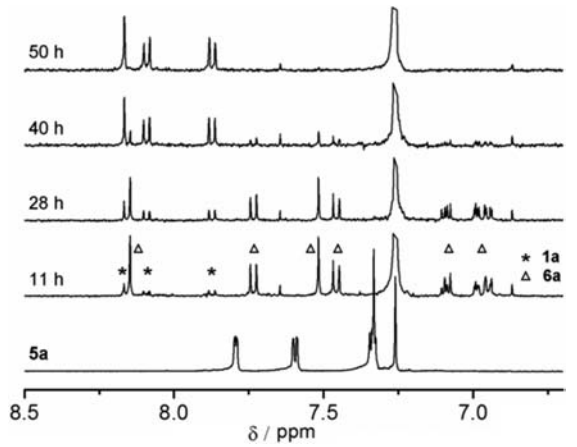

Figure 3. Monitoring of a reaction of **5a** upon photoirradiation in the presence of I_2 by ^1H NMR spectroscopy.

Scheme 2. Plausible Mechanism of the Double Cyclization from **5a** to **1a**

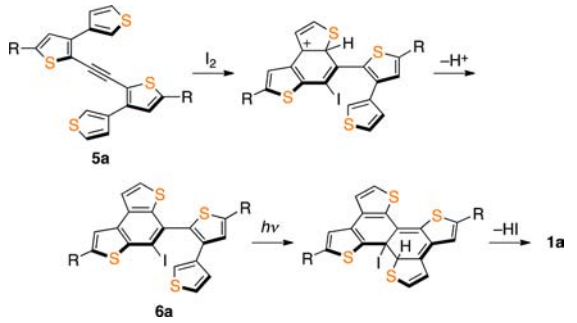

double cyclized compound **1a**. The crystal structure analysis demonstrated that the intermediate is a monocyclized product **6a** consisting of a tricyclic dithienobenzene skeleton with an iodine atom (Figure 2b). Thus, the initial step is likely an electrophilic monocyclization mediated by I_2 to give the intermediate **6a**.[10] The photoirradiation likely promotes the second electrocyclization, which is followed by aromatization to construct the TTN skeleton (Scheme 2).

The availability of the regiospecifically bis-silylated TTN derivatives **1a** and **1b** enabled us to produce a series of cruciform π-extended derivatives with electron-donating (D) and electron-accepting (A) aryl groups in specific positions (Schemes S1 and S2, Supporting Information). Thus, the Pd-catalyzed direct C–H arylation[11] of **1a** or **1b** with 3,4-dioctyloxyphenyl iodide followed by desilylation and the second direct C–H arylation with 3,5-bis(trifluoromethyl)phenyl iodide gave the DADA-type **2** and

(10) The possibility that this reaction is promoted by iodine radical or through the charge-transfer process is not ruled out at this stage.

(11) Ueda, K.; Yanagisawa, S.; Yamaguchi, J.; Itami, K. *Angew. Chem., Int. Ed.* **2010**, *49*, 8946.

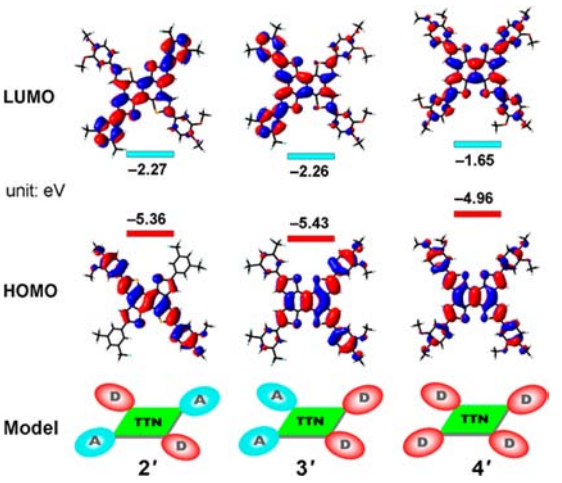

Figure 4. Pictorial presentations of Kohn–Sham HOMOs and LUMOs with their energy levels for models **2′**–**4′**, calculated at the B3LYP/6-31G* level.

DDAA-type **3**, respectively, in 33 and 44% overall yields in three steps. In essentially the same manner, the 3,4-dioctyloxyphenyl-substituted DDDD-type compound **4** was also successfully prepared.

The cruciform compounds **2**–**4** are a suitable set for studying the potentials of the TTN core as a π-conjugated intersection. To investigate the impact of the π-extension modes on the electronic structures, we first conducted the DFT calculations at the B3LYP/6-31G* level using the model compounds **2′**–**4′**, in which the octyloxy groups of **2**–**4** are replaced with methoxy groups.[12] The HOMOs and LUMOs of **2′** and **3′** are mainly delocalized over the dialkoxyphenyl and bis(trifluoromethyl)phenyl moieties, respectively, through the TTN core skeletons (Figure 4). The π-extension modes, namely, the diagonal or chevron-shaped extension, only have a subtle effect on their energy levels. For **4′** with the four electron-donating groups, both the HOMO and LUMO are delocalized over the entire framework, resulting in the increased energy levels compared to those of **2′** and **3′**. These electronic structures demonstrated that the TTN core is an effective intersection that can extend the π-conjugation on demand.

These discussions are supported by cyclic voltammetry, which were measured in THF for reduction and in *o*-dichlorobenzene for oxidation (Figures S4 and S5, Supporting Information). In the reduction process, both **2** and **3** showed two reversible redox waves with $E_{1/2}$ at around −2.13 and −2.31 V (vs Fc/Fc^+), while **4** only showed an irreversible reduction wave with higher cathodic peak potential (E_{pc}) of −2.60 V. In the oxidation process, **2** showed two reversible redox waves, while **3** and **4** only showed an irreversible oxidation wave. Their first anodic peak potentials (E_{pa}) are in the order of **4** (+0.34 V),

(12) Frisch, M. J. et al. Gaussian 09, Rev. C.01. Gaussian, Inc., Wallingford, CT, 2009. See the Supporting Information for the full reference.

2 (+0.49 V) and **3** (+0.60 V). These trends are qualitatively in agreement with their HOMO and LUMO energy levels in Figure 4.

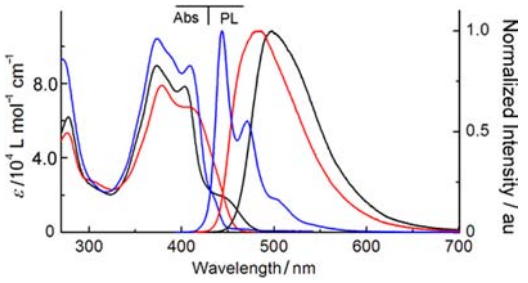

Figure 5. UV−vis absorption and fluorescence spectra for **2** (black), **3** (red), and **4** (blue) in THF.

Table 1. Photophysical Properties of TTN Derivatives **2**−**4**

	THF solution				fibers	
compd	λ_{abs}[a] (nm)	ε_{max} ($M^{-1}cm^{-1}$)	λ_{em}[b] (nm)	Φ_F[c]	λ_{em}[b] (nm)	Φ_F[c]
2	373	89600	497	0.10	535	0.04
	448 (sh)	17800				
3	378	78900	483	0.15	561	0.05
4	373	104000	444	0.08	551	0.06

[a] Only the longest absorption maxima are shown. [b] Emission maxima upon excitation at the absorption maximum wavelengths. [c] Absolute quantum yield determined by a calibrated integrating sphere system within errors of ±3%.

To further investigate the structure−property relationship, we next evaluated the photophysical properties of **2**−**4** (Figure 5 and Table 1). In the absorption spectra in THF, while all the derivatives have the strongest absorption bands around 380 nm, the longest wavelength bands of these compounds depend on the modes of the π-extension. The diagonal extension in **2** produces a distinct shoulder band at 448 nm, whereas the chevron-shaped or four-directional π-extension in **3** and **4** only results in obscure shoulder bands. The TD−DFT calculations (Supporting Information) suggested that the shoulder band in **2** is assignable to the electronic transition from the HOMO to LUMO, which are orthogonally extended to each other. In the fluorescence spectra in THF, while the four-directionally extended **4** showed a structured emission, **2** and **3** exhibited broad emission bands at the longer wavelengths. The difference in the emission maxima between **2** and **4** exceeds 50 nm, demonstrating the impact of the π-extension modes. As for the solvent effects, while **4** did not show any solvent-dependence, **2** and **3** showed slight red-shifts of the emission bands from toluene to THF by 13 and 26 nm, respectively.

All of the π-extended TTN derivatives **2**−**4** exhibited strong self-assembling properties. Even their diluted solutions in tetrachloroethane with the concentration of

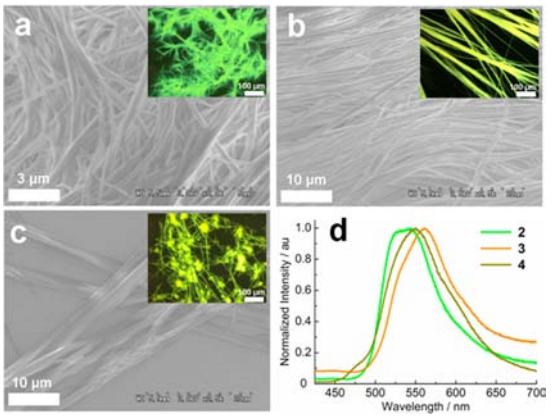

Figure 6. SEM images of (a) **2**, (b) **3**, and (c) **4**. The inset figures are fluorescence microscopy images in which the scale bars indicate 100 μm. (d) Fluorescence spectra of the fibers of **2**−**4**.

$\sim 10^{-3}$ M started to form aggregates upon reducing the temperature below 60 °C (Supporting Information). Upon slow evaporation of their THF solutions (5×10^{-5} M) at room temperature, they gradually formed yellow nano/microfibers. Their scanning electronic microscopy (SEM) images showed the formation of smooth fibers of **2** with widths of 0.5−1 μm and thicknesses of 100−200 nm, while **3** and **4** formed hierarchically assembled fibers with the fibrous unit diameter of about 200 nm (Figure 6). The fibers of **3** and **4** emitted a yellow fluorescence with the peaks centered at 561 and 551 nm, respectively, while the fibers of **2** emitted a green fluorescence with a broad emission band around 525−544 nm. The difference in their emission maxima should be attributed to the different packing structures in their nanostructures (Supporting Information).

In summary, we have developed an efficient and facile one-pot sequential double cyclization for the construction of a planar tetrathienonaphthalene (TTN) skeleton. The TTN derivatives showed the effective extension of π-conjugation on demand and exhibited strong aggregation properties, indicative of a significant potential as a cruciform scaffold for nanostructured π-electron materials.

Acknowledgment. This work was supported by CREST, JST, and a Grant-in-Aid for Young Scientists (B) (24750038). We thank Dr. H. Yoshikawa and Prof. K. Awaga (Nagoya University) for use of the scanning electronic microscopy (SEM) and T. Hikage (High Intensity X-ray Diffraction Laboratory, Nagoya University) for powder XRD measurements.

Supporting Information Available. Experimental procedures, X-ray crystallographic details, photophysical properties, theoretical calculations, and aggregation properties. This material is available free of charge via the Internet at http://pubs.acs.org.

The authors declare no competing financial interest.